Bacteria Counting with Impedance Spectroscopy in a Micro Probe Station

Mats Jönsson,[†] Ken Welch,[†] Sven Hamp,[‡] and Maria Strømme*,[†]

Department of Engineering Sciences, The Ångström Laboratory, Uppsala University, Box 534, SE-751 21 Uppsala, Sweden, and Department of Biology and Chemical Engineering, Mälardalen University, Box 325, SE-631 05, Eskilstuna, Sweden

Received: January 9, 2006; In Final Form: March 21, 2006

A method to quantify the density of viable biological cells in suspensions is presented. The method is implemented by low-frequency impedance spectroscopy and based on the finding that immobilized ions are released to move freely in the surrounding suspension when viable *Escherichia coli* cells are killed by a heat shock. The presented results show that an amount of ions corresponding to $\sim 2 \times 10^8$ unit charges are released per viable bacterium killed. A micro probe station with coplanar Ti electrodes was electrically characterized and used as a measuring unit for the impedance spectroscopy recordings. This unit is compatible with common microfabrication techniques and should enable the presented method to be employed using a flow-cell device for viable bacteria counting in miniaturized on-line monitoring systems.

1. Introduction

Processes for manufacturing proteins are, today, based on microorganisms in suspensions of nutrients. Monitoring of such processes, in particular those that involve fermentation of genetically modified bacteria, poses particular challenges for control and regulation. For example, these processes are very sensitive to aeration since lack of dissolved oxygen will result in process failure within a few seconds. Consequently, the bacterial cultures must be constantly observed and successively regulated by different additives or energy input. Monitored data are compared to standard process models and adjustments to the process can be made. Several methods of analysis for such monitoring have been suggested, comprehensively reviewed by Schügerl,[1] including, e.g., analysis of dissolved oxygen tension,[2] pH measurements,[3] fermentation gas analysis,[4] viable count (VC) tests,[5] optical density (OD) measurements,[4] and medium conductivity[6] recordings.

For standard on-line monitoring of bacterium cell density, the OD measurement technique has hitherto been preferred because of its rapid response. This method is, however, rather imprecise in comparison to, e.g., the much more time-consuming VC method.[5] In addition, it has an inherent weakness in not producing quality data related to the state of growth of the cells. Such data are of particular importance when cultures are induced to produce proteins. Both viable and dead cells will give a contribution to the OD measurements, thereby confusing the real state of the microbial cell culture. Also, the effect of the accumulating proteins makes the optical properties of the protein-producing cells deviate strongly from noninduced viable cells. In production processes OD data are used in combination with data from an ideal process to predict the state of the producing culture. By experience, however, such comparisons are uncertain and cannot be used for process development. Hence, there is great need for other rapid and cost-efficient techniques for measuring bacterium cell density that can be used independently or in combination with OD measurements.

Electrokinetic methods have the potential of becoming valuable tools in the development of such techniques. For example, fungus cells such as yeast have been studied thoroughly, and viability[7] and cell growth[8] of known samples have been investigated. Transient capacitance and conductance measurements have been exploited for estimations of the biomass concentration of *Escherichia coli* (*E. coli*) in which the difference in the rate of dielectrophoretic cell collection at electrode arrays is used to determine the concentration of the cell suspensions. Positioning and separation of cells by dielectrophoresis (DEP) and electrorotation in an electric ac field gradient have been presented.[9−11] DEP is commonly used to selectively trap cells. The dielectrophoretic force on a cell depends on the shape and size of the cell, the electric field gradient, and the relation between the permittivity of the sample and the surrounding medium. The detection of the manipulated sample is either done optically or a dielectric sensor is integrated in the device. Optical detection using a microscope is limited to visible sample sizes and the possibility to label the sample cells with e.g. fluorescent markers. The drawbacks of this electrokinetic method are that the magnitude of the dielectrophoretic force is local and decreases with the size of the cells and that the buffer conductivity has to be kept low. In a concentrated suspension the cell−cell interactions strongly dominate the force conditions. Electrorotation and traveling wave methods can enhance the effect of dielectrophoretic forces but low-concentration suspensions are needed in order to avoid disturbing effects from the above-mentioned interactions.

Electrokinetic studies on living matter, using impedance spectroscopy, have been performed since the early 20th century; see e.g. ref 12 and references therein. The impedance response of cells has been investigated, and models have been developed to account for the measured behavior.[13−20] Impedance spectroscopy has been utilized to monitor the biomass concentration and to study the sporulation of *Bacillus thuringensis*,[21] and transient capacitance measurements at frequencies in the β-dispersion region (MHz) were used to determine changes in permittivity during growth in order to identify culture phases. A similar procedure was employed to perform biomass mea-

* To whom correspondence should be addressed.
[†] Uppsala University.
[‡] Mälardalen University.

10.1021/jp060148q CCC: $33.50
Published on Web 04/22/2006

surements of *Lactobacillus casei* in high-conductivity suspensions.[22] Determination of bacterial particle conductivity by separate measurements of particle and medium suspensions using a conventional conductivity meter have also been presented.[6] As well, the metabolism of living *E. coli* cells has been monitored by impedance spectroscopy, showing that the transfer of ions across the cell membrane of living cells results in a higher conductivity in the suspension surrounding the cells than in an equivalent suspension containing dead cells from which all loosely bound ionic species were removed.[23]

The present work puts forward that impedance spectroscopy analysis of the response pertaining to a suspension containing the investigated cells before and after induced cell death can be used to determine the number of *viable* cells in the bacterial culture under study. The scientific basis for such an analysis is that the cell membrane becomes permeable when the cell dies, resulting in the disappearance of the transmembrane potential.[24] Ions that are forced to reside in the interior of the viable cell by this potential should be able to diffuse out to the medium surrounding the cell when it dies, thus increasing the free ion concentration in the surrounding medium.

There are three aims of this work. *First*, this work aims to show that there is a difference in the free charge carrier concentration—and thus in the conductivity—of the medium surrounding viable and dead *E. coli* cells, and *second*, it aims to show how this difference may be used for viable cell counting.

Presently, there is an urge to design integrated miniaturized analysis systems, so-called micro total analysis systems (μTAS), because of the benefits related to small sample consumption, faster analysis, low cost, and the possibilities to integrate functions such as transport, manipulation, positioning, separation, and detection in one chip.

To take a step toward meeting this urge, a micro probe station that may be used in a future flow-cell device for viable bacteria counting is utilized in the impedance spectroscopy measurements. The *third* aim of the present work is, thus, to perform an electrical characterization of this micro probe station.

2. Materials and Methods

2.1. Bacteria. *E. coli* bacteria of genetically modified strain BL21 were cultured batchwise in LB (Luria-Bertani) broth medium[25] at 37 °C, 30% dissolved oxygen, and pH 7.0 using a 250 l fermenter (Belach AB). Bacterial growth was monitored by OD measurements according to the procedure described below. Harvest and sampling was done at an OD of 1.24 for the stock suspension.

2.2. Optical Density Measurements. The turbidity of the sample gives a measure of the total number of cells (viable and dead). This quantity is obtained by light absorbance measurements at 600 nm (A_{600}) using a spectrophotometer (Milton Roy, Spectronic 601).[26] The OD unit is calculated as $\log(I_0/I)$, where I_0 and I are the incident and the transmitted (unscattered) light intensities, respectively.

2.3. Viable Count. Determination of the amount of viable cells in the suspensions was performed by VC.[25] Serial dilution of the stock suspension in phosphate buffered saline (PBS) was done in sequence to concentrations of 10^{-6}, 10^{-7}, and 10^{-8} of the stock concentration. From each of the three diluted sample solutions 100 μL was dispensed onto a separate agar plate and incubated at 31 °C overnight. Then the number of colony-forming units (cfu) was counted. The stock suspension was washed three times with glucose buffer (15 g/L) prior to analysis. The analysis showed that the stock suspension contained 27×10^8 cfu/mL with an uncertainty of ~10%.

2.4. *E. coli* Sample Preparation and Characterization. The (main) stock *E. coli* suspension was diluted with a glucose (buffer) solution (15 g/L) to three different concentrations viz. 1.7×10^8, 3.4×10^8, and 6.8×10^8 viable *E. coli* bacteria per millilter of buffer respectively, as obtained from VC. A part of the volume of each concentration was heated to 60 °C for 20 min in order to kill the bacteria. A subsequent VC on these solutions showed that there were indeed no viable bacteria present after the heat treatment.

2.5. Impedance Spectroscopy. In impedance spectroscopy, a sinusoidal voltage is applied across a sample localized between two electrodes in a probe station and the frequency of the voltage is scanned from a maximum to a minimum value. The measured current response due to charged species present in the sample can be interpreted in terms of several interrelated complex frequency-dependent parameters such as impedance, conductance, capacitance, and dielectric permittivity. For example, the complex permittivity ϵ^* of a sample is obtained from the measured capacitance C as

$$\epsilon^* = \epsilon' + i\epsilon'' = \frac{C}{C_0} \tag{1}$$

where C_0 is the capacitance of the empty probe station and ϵ' and ϵ'' are the real and imaginary parts of the permittivity, respectively. For a parallel plate electrode probe station $C_0 = \epsilon_0 A/d$, where A and d are the electrode area and electrode separation distance, respectively, and ϵ_0 is the permittivity of free space (8.854×10^{-14} F/cm).

In this work we focus on the analysis of the real part, σ', of the complex conductivity, σ, which is related to the real part, G', of the measured conductance and to the imaginary part, ϵ'', of the dielectric permittivity as

$$\sigma' = \frac{d}{A}G' = \omega\epsilon_0\epsilon'' \tag{2}$$

Here ω is the angular frequency.

At high frequencies, the movable ions in a sample will only have time to travel a very short distance before the sign of the applied sinusoidal field is changed and the ions are forced to change their direction of motion. Thus, at high enough frequencies, the ions will be able to move unhindered by the electrodes as if they were free. The conductivity associated with this dc-like motion can be expressed as

$$\sigma_{dc} = \frac{nq^2D}{kT} \tag{3}$$

where n is the concentration of carrier ions, q is the ionic charge, q is the ion diffusion coefficient, and kT represents the thermal energy.

At lower frequencies the movement of ions is hindered by the electrodes—a phenomenon referred to as electrode polarization—and under certain circumstances, such that the electric fields created by charge separation near the electrode surfaces do not induce nonlinear effects,[27,28] the charge carrier concentration can be extracted from the permittivity spectrum using the following relation[29]

$$n = \left(\frac{\sigma_{dc}}{\sqrt{(X-1)}\epsilon_0\epsilon_s'\omega_X}\right)^4 \frac{\epsilon_0\epsilon_s' kT}{q^2 d^2} \tag{4}$$

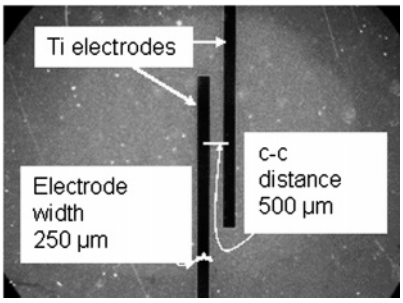

Figure 1. Micro probe station with Ti electrodes of 250 μm width, 3 mm length, and 500 μm center-to-center spacing.

Here ϵ_s' is the real part of the dielectric permittivity in the high-frequency region where σ' is dominated by dc-like ion conduction and ω_X is the angular frequency for which $\epsilon'(\omega_X) = X\epsilon_s'$.

2.5.1. Micro Probe Station and Measurement Equipment. The microfabrication of the micro probe station (MPS) was done by a photolithographic process of a Ti layer on a glass substrate. The electrode structures were manufactured in a clean room facility. The substrate used was standard soda-lime glass, with lateral dimensions 76 × 35 mm and a thickness of 2 mm, which was cleaned using the standard RCA-cleaning procedure.[30] The Ti layer was deposited by sputtering Ti onto the glass to form a layer with a thickness of 0.15 μm. Photolithography of positive photoresist (Shipley 1813) was used for patterning and the excess Ti was removed by etching in buffered HF solution (5% v/v HF buffered with ammonium fluoride). The photoresist was removed in acetone and the slide was spin-dried. Electrical connection to the electrodes was achieved by bonding wires to the contact pads using conductive epoxy glue. The MPS is shown in the photography of Figure 1. The coplanar Ti electrodes have a width of 250 μm, a length of 3 mm, and a center-to-center spacing of 500 μm.

A Novocontrol broadband dielectric converter (Novocontrol GMBH, Hundsangen, Germany) and a Solartron 1260 frequency response analyzer (Solartron Instruments, Hampshire, U.K.) were attached to the MPS via 50 Ω coaxial cables and used for the impedance spectroscopy measurements performed in the present work.

2.5.2. Measurement Procedure. A 20 μL droplet of the sample to be tested was dispensed onto the electrode spot. A glass cover was put on top of the setup to avoid evaporation during the impedance spectroscopy measurements. All measurements were performed at room temperature with an ac voltage amplitude of 0.25 V and the frequency was scanned from 10^5 to 10^{-1} Hz.

2.5.3. Characterization of Micro Probe Station. To extract conductivity data from impedance spectroscopy measurement using eq 2, knowledge about functional parameters of the MPS, such as the effective electrode area and electrode distance, must be accessible.

The MPS is characterized by recording impedance spectra for deionized water in the MPS as well as in a reference parallel-plate station (PPS) consisting of cylindrical gold electrodes with a diameter of 10.4 mm and an electrode separation of 1.5 mm. When the real parts of the high-frequency permittivity of the two measurements are matched, the effective electrode separation to area ratio, d/A, can be determined. Further, when the charge carrier concentration is first calculated from the spectrum recorded on the PPS (with known d), an effective d for the MPS can be obtained by employing eq 4.

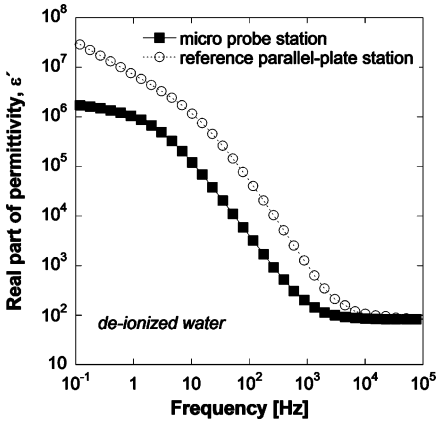

Figure 2. Real part of permittivity vs frequency for deionized water recorded in the micro probe station and in the reference parallel-plate station.

3. Results and Discussions

3.1. Characterization of Micro Probe Station. Figure 2 shows the real part of the dielectric permittivity of deionized water extracted from the frequency-dependent capacitance recorded on the reference PPS and the MPS for frequencies ranging from 10^{-1} to 10^5 Hz. In a comparison of the two response curves, it can be seen that the low-frequency behavior, pertaining to electrode polarizations, differs between the electrodes. This discrepancy is due to a dissimilar nano- and microscale roughness and, thus, fractal surface dimension of the electrodes.[31] The fact that the MPS electrodes induce an ideal permittivity response for electrodes with a fractal surface dimension close to 2, whereas the reference PPS electrodes induce a power-law behavior in the measured real part of the permittivity, indicates that the nano- and microstructure of the former ones are smoother.[31]

At frequencies in the 10^4 to 10^5 Hz range a water permittivity of ∼80 is obtained using the PPS, in excellent agreement with literature values.[32] For the high-frequency permittivity obtained from the MPS to match this value, d/A was determined to be 0.239 mm^{-1}. Knowledge about this ratio is sufficient to be able to extract correct σ' values from the measured conductance (eq 2). However, to obtain more detailed information about the ion transport path in the MPS, the effective electrode spacing d is also determined by first calculating the charge carrier density from the PPS reference measurements and then using this value to extract d for the MPS using eq 4.

The above analysis is summarized in Figure 3. From panel a—displaying the real part of the deionized water conductivity in the PPS—the σ_{dc} value to be used in eq 4 for the calculation of n is extracted from the plateau region between ∼10^2 and 10^5 Hz. Below this frequency region σ' drops as electrode polarization dominates the charge transport process. The extracted σ_{dc} together with $\epsilon_s' = 80$ are inserted into eq 4 and the equation is evaluated for a range of ω_X values. The resulting n is also displayed in panel a. The approximately constant n region around 10^3 Hz signifies the region of validity for eq 4. At lower frequencies, the linearity assumption for the internally generated electric fields no longer holds and an incorrect rise in n toward lower frequencies results. From the approximately constant n region, a charge carrier concentration for the deionized water of ∼4×10^{16} unit charges per cm^3 is extracted. This value is significantly higher than the 6×10^{13} H^+ ions per cm^3 that are ideally present in pure water at neutral pH. The reason for the higher conductivity and, thus, charge carrier concentration observed in reality is due to dissolved CO_2, forming carbonic

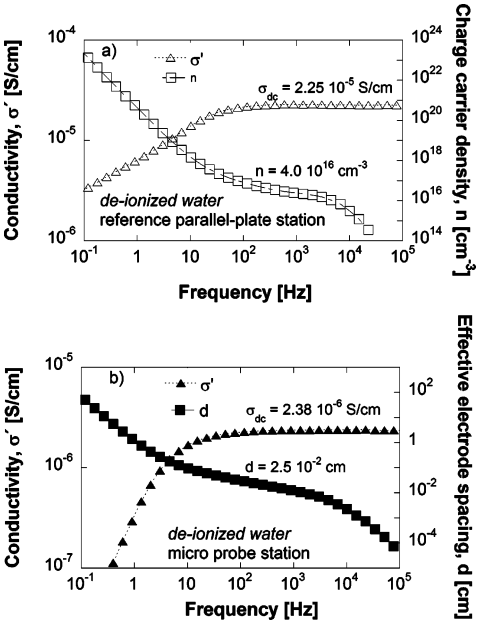

Figure 3. (a) Real part of deionized water conductivity as measured in the reference parallel-plate station and charge carrier concentration calculated from eq 4. The extracted σ_{dc} and n values are also displayed. (b) Real part of deionized water conductivity as measured in the micro probe station and effective electrode separation calculated from eq 4. The extracted σ_{dc} and d values are also displayed.

acid that dissociates into bicarbonate ions, and subsequently lowering the pH of water according to

$$CO_2 + H_2O \rightarrow H_2CO_3 \rightarrow H^+ + HCO_3^- \qquad (5)$$

Inserting the obtained σ_{dc} and n values into eq 3 gives a diffusion coefficient of $\sim 8.8 \times 10^{-5}$ cm^2/s, which is slightly lower than the literature value for proton diffusion in water (9.31×10^{-5} cm^2/s).[33] This lowering is most certainly due to the fact that the measured n value in addition to protons also contains a contribution from the slower bicarbonate ions (1.185×10^{-5} cm^2/s)[31] and possibly also other larger ions inadvertently present in the deionized water.

Knowing n and ϵ_s', the effective electrode separation of the MPS is readily extracted from eq 4. Panel b shows the real part of the deionized water conductivity in the MPS, from which $\sigma_{dc} = 2.38 \times 10^{-6}$ S/cm is obtained, as well as the calculated d. Just as for the calculated n values, an approximately constant d region is visible in the plot, signifying the region of validity for eq 4. The extracted d value is ~ 250 μm and, thus, equivalent to the electrode spacing in the MPS (Figure 1), rather than the center-to-center distance of 500 μm. This shows that the electric field is strongest along the surface between the electrodes and, thus, that the major contribution to the measured response comes from ions moving in the vicinity of the surface.

When the diffusion coefficient for the charge carriers in deionized water in the MPS is calculated, a value of $\sim 9.3 \times 10^{-6}$ cm^2/s is obtained, which is almost an order of magnitude lower than that in the PPS. This low value of the diffusion coefficient is most likely due to interactions between the charge carriers and the hydrophilic surface of the glass substrate between the electrodes.

Once the MPS was characterized, the results of the *E. coli* bacteria containing solutions could be evaluated.

3.2. *E. coli* Conductivity Measurements. Figure 4 shows the conductivity curves for the glucose buffer and the three different viable and dead *E. coli* suspensions. The inset of this figure displays a magnification of the high-frequency part of the *E. coli* suspension conductivities. First, it can be noticed that the conductivity of the glucose buffer is lowered by a factor of ~ 2.4 with respect to that of deionized water (cf. Figure 3b). This lowering pertains to the viscosity increase resulting from dissolving glucose in water.[34] Second, it is obvious from the figure that killing the bacteria leads to an increase in the conductivity. The heat treatment does not imply any addition to the total number of ions in the suspension. Thus, the increased conductivity must stem from ions initially localized in the interior of the cell being released and free to move under the action of the applied electric field.

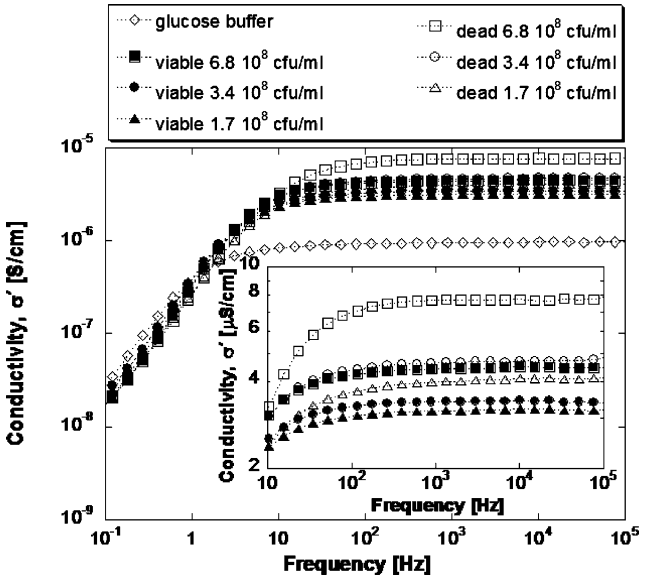

Figure 4. Conductivity curves for glucose buffer and for three different concentrations of viable and dead *E. coli* solutions. The inset shows a magnification of the high-frequency part of the *E. coli* solution conductivities.

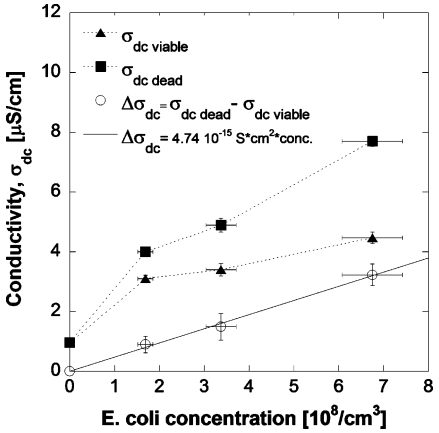

Figure 5. The dc conductivities for samples of viable ($\sigma_{dcviable}$) and dead (σ_{dcdead}) bacteria vs bacterial concentration. The conductivity difference ($\Delta\sigma_{dc} = \sigma_{dcdead} - \sigma_{dcviable}$) and its linear curve fit are also displayed. The horizontal error bars signify the uncertainty of the viable count measurements while the vertical bars reflect the uncertainty pertaining to the extraction of the dc conductivity from impedance spectroscopy.

In Figure 5 the dc conductivities, extracted from the conduction plateaus in Figure 4, are shown vs bacterial concentration for both samples of viable ($\sigma_{dcviable}$) and dead (σ_{dcdead}) cells. Included in this figure is also the conductivity difference, $\Delta\sigma_{dc} = \sigma_{dcdead} - \sigma_{dcviable}$, which seems to have an approximately linear increase with increasing bacterial concentration. A linear curve fit to the data shows that this increase is $\sim 4.7 \times 10^{-15}$

S/cm for each bacterium added per cm^3 solution. With use of eq 3 and the diffusion coefficient calculated for the charge carriers in the MPS, reduced by a factor of 2.4 to take into account the viscosity increase created by the glucose addition, the conductivity increase is equivalent to an increase in movable ion concentration of $\sim 1.9 \times 10^8$ unit charges per viable bacterium. This number corresponds well to the number of released ions that may be estimated from measurements of the conductivity of the interior of viable *E. coli* cells[35] and assuming that the interior of the cells take on the conductivity of the surrounding medium when the cells die.

The approximate linearity in $\Delta\sigma_{dc}$ vs bacterial concentration may form a new and simple means of viable cell counting that does not require OD or VC analyses. With measurement of the dc conductivity in a suspension of the material to be tested before and after heat treatment, the conductivity difference should give an assessment of the number of viable bacteria initially present.

It is worth noticing that the method of estimating the number of viable cells presented in the current work differs from an earlier suggested method of employing impedance spectroscopy to monitor the number of viable cells in a suspension.[23] In this earlier publication it was shown that the number of ions passing in and out from a living cell, due to the normal cell metabolism, induced a slightly higher conductivity in the suspension surrounding the cells than did dead cells that had been washed and, thus, deprived of their released ionic content prior to the impedance measurements.

4. Summary and Conclusion

The current work presents a new method to quantify the amount of viable biological cells in suspensions. Conductivity data, obtained from low-frequency ($10^{-1}-10^5$ Hz) impedance spectroscopy, showed that the free charge carrier concentration in a suspension of viable *E. coli* bacteria increased linearly with bacterial concentration upon killing the bacteria by heat shock. The increase was attributed to the release of ions from the interior of the cells as the cells were killed. These freed ions can move freely under the action of the applied electric field. By viable count measurements the increase could be quantified to $\sim 1.9 \times 10^8$ free ions of unit charges per bacterium. An analogous result is expected also by the application of other means of killing the bacteria, as long as it does not involve any change of the total ionic content of the suspension.

The scientific basis for such an analysis is that the cell membrane becomes permeable when the cell dies, resulting in the disappearance of the transmembrane potential.[24] Ions that are forced to reside in the interior of the viable cell by this potential should be able to diffuse out to the medium surrounding the cell when it dies, thus increasing the free ion concentration in the surrounding medium.

To lay the foundation for a simple analysis and detection systems, a micro probe station suitable for use in a flow-cell device for viable bacteria counting was employed as the measuring unit for the impedance spectroscopy recordings. The unit was characterized electrically in order to make quantitative analysis of the recorded data possible. The coplanar microelectrodes in the unit are compatible with common microfabrication techniques, which should enable for the presented method to be implemented in miniaturized on-line monitoring systems.

The main application in mind for the presented method is selective biomass measurements, but the method is versatile and, thus, also suitable for general electrokinetic studies of living matter and particles as the employed procedure is reliable and easy to apply.

Acknowledgment. The authors thank Pär Fernkvist at the Department of Surface Biotechnology, Uppsala University, for help with the bioprocessing. As well, Fredrik Aldaeus, Lars Erik Johansson, and Gunnar Jonsson are gratefully acknowledged for fruitful discussions. One of the authors (M.S.) is a Royal Swedish Academy of Sciences Research Fellow and would like to thank the Academy (KVA) for their support. The Swedish Foundation of Strategic Research as well as the Knut and Alice Wallenberg Foundation are also acknowledged for financially supporting our multidisciplinary research.

References and Notes

(1) Schügerl, K. *J. Biotechnol.* **2001**, *85*, 149−173.
(2) Li, X. L.; Robbins, J. W.; Taylor, K. B. *J. Ind. Microbiol.* **1992**, *9*, 1−9.
(3) Alba, M. J. G.; Calvo, E. G. *J. Biotechnol.* **2000**, *84*, 107−118.
(4) Lin, H. Y.; Mathiszik, B.; Xu, B.; Enfors, S. O.; Neubauer, P. *Biotechnol. Bioeng.* **2002**, *73*, 347−357.
(5) Bridges, B. A.; Ereira, S. *J. Bacteriol.* **1998**, *180*, 2906−2910.
(6) Yunus, Z.; Mason, V.; Verduzco-Luque, C. E.; Markx, G. H. *J. Microbiol. Methods* **2002**, *51*, 401−406.
(7) Markx, G. H.; Talary, M. S.; Pethig R. *J. Biotechnol.* **1994**, *32*, 29−37.
(8) Asami, K. M.; Gheorghiu, E.; Yonezawa, T. *Biochim. Biophys. Acta* **1998**, *1381*, 234−240.
(9) Betts, W. B. *Trends Food. Sci. Technol*. **1995**, *6*, 51−58.
(10) Goater, A. D.; Burt, J. P. H.; Pethig, R. *J. Phys. D: Appl. Phys*. **1997**, *30*, L65−L69.
(11) Brown, A. P.; Betts, W. B.; Harrison, A. B.; O'Neill, J. G. *Biosens. Bioelectron.* **1999**, *14*, 341−351.
(12) Riu, P. J., Rosell, J., Bragós, R., Casas, O., Eds. *Electrical bioimpedance methods: Applications to medicine and biotechnology*; Annals of the New York Academy of Sciences; New York Academy of Sciences: New York, 1999; Vol. 873.
(13) Schwan, H. P. *Adv. Biol. Med. Phys.* **1957**, *5*, 147−209.
(14) Gheorghiu, E. *J. Phys. A: Math. Gen.* **1994**, *27*, 3883−3893.
(15) Gheorghiu, E. *Bioelectrochem. Bioenerg.* **1996**, *40*, 133−139.
(16) Zimmermann, U.; Neil, G. A. *Electromanipulation of cells*; CRC Press: New York, 1996.
(17) Gheorghiu, E.; Asami, K. *Bioelectrochem. Bioenerg.* **1998**, *45*, 139−143.
(18) Gimsa, J.; Wachner, D. *Biophys. J.* **1998**, *75*, 1107−1116.
(19) Prodan, C.; Prodan, E. *J. Phys. D: Appl. Phys.* **1999**, *32*, 335−343.
(20) Markx, G. H.; Davey, C. L. *Enzyme Microb. Technol*. **1999**, *25*, 161−171.
(21) Sarrafzadeh, M. H.; Belloy, L.; Esteban, G.; Navarro, J. M.; Ghommidh, C. *Biotechnol. Lett.* **2005**, *27*, 511−517.
(22) Arnoux, A. S.; Preziosi-Belloy, L.; Esteban, G.; Teissier, P.; Ghommidh, C. *Biotechnol. Lett.* **2005**, *27*, 1551−1557.
(23) Gómez, R.; Bashir, R.; Bhunia. A. K. *Sens. Actuators, B* **2002**, *86*, 198−208
(24) Pethig, R.; Markx, G. H. *Trends Biotechnol.* **1997**, *15*, 426−432.
(25) Sambrook, J.; Fritsch, E. F.; Maniatis, T. *Molecular cloning: A laboratory manual. 2nd edn.*; Cold Spring Harbour Laboratory Press: New York, 1989.
(26) Madigan, M. T.; Martinko, J. M.; Parker, J.; Brock, T. D. *Brock biology of microorganisms*; Prentice Hall International: London, 1998; pp 154−160.
(27) Coelho, R. *Rev. Phys. Appl.* **1983**, *18*, 137−146.
(28) Schütt, H. J.; Gerdes, E. *J. Non-Cryst. Solids* **1992**, *144*, 1−13.
(29) Niklasson, G. A.; Jonsson, A. K.; Strømme, M. Impedance response of electrochromic materials and devices. In *Impedance Spectroscopy 2nd ed.*; Barsoukov, Y., MacDonald, J. R., Eds.; Wiley: New York, 2005; pp 302−326.
(30) Madou, M. J. *Fundamentals of microfabrication*; CRC Press: Boca Raton, FL, 2005; p 10.
(31) Bates, J. B.; Chu, Y. T.; Stribling, W. T. *Phys. Rev. Lett.* **1988**, *60*, 627−630.
(32) Archer, D. G.; Wang, P. M. *J. Phys. Chem. Ref. Data* **1990**, *19*, 371−411.
(33) Lide, D. R., Ed. *CRC Handbook of Chemistry and Physics. 85th ed.*; CRC Press: Boca Raton, FL, 2004.
(34) Soesanto, T.; Williams, M. C. *J. Phys. Chem.* **1981**, *85*, 3338−3341.
(35) Suehiro, J.; Hamada, R.; Noutomi, D.; Shutou, M.; Hara, M. *J. Electrostat.* **2003**, *57*, 157−168.